

## Photochemistry of Trimethyltin Iodide in Polar Media: Orbital Parentage and Observed Reactivity

Jinquan Dong, P. Sujatha Devi, D. Sunil, Edgar Mendoza, and Harry D. Gafney\*

Department of Chemistry, City University of New York, Queens College, Flushing, New York, 11367

Received January 15, 2001

$(\text{CH}_3)_3\text{SnI}$  exists as individual tetrahedral molecules in hexane but reacts with the silanol moieties present on the surface of porous glass and with the hydroxyl group of ethanol and hexanol to form five-coordinate adducts. With the exception of slight shifts to higher energy, formation of the adduct has little effect on the electronic spectrum of the complex, and the wavelength and  $\text{O}_2$  dependencies of the quantum yield of  $(\text{CH}_3)_3\text{SnI}$  disappearance indicate that the photochemistry of the complex initiates from the ligand-to-metal charge-transfer (LMCT) state populated on absorption in each medium. Nevertheless, 254 nm excitation in hexane leads to  $\text{I}_2$  and  $((\text{CH}_3)_3\text{Sn})_2$ , whereas excitation of the five-coordinate adduct on the glass surface leads to  $\text{I}_2$ ,  $\text{I}_3^-$ ,  $((\text{CH}_3)_3\text{Sn})_2$ , and  $(\text{CH}_3)_3\text{Sn}-\text{OSi}\equiv$  ( $\text{OSi}\equiv$  represents a surface siloxy), while in ethanol,  $\text{I}_3^-$  is the only detectable product. Regardless of the medium, the ground state is polarized and population of the LMCT state creates a more uniform charge distribution from which homolytic cleavage of the  $(\text{CH}_3)_3\text{Sn}-\text{I}$  bond is the dominant reaction pathway in each medium. In hexane, the  $(\text{CH}_3)_3\text{Sn}^\bullet$  and  $\text{I}^\bullet$  radicals couple to form  $((\text{CH}_3)_3\text{Sn})_2$  and  $\text{I}_2$ , whereas adsorbed onto the glass, a fraction of the radical pairs thermalize via electron transfer to form  $\text{I}_3^-$  and a surface-bound  $(\text{CH}_3)_3\text{Sn}-\text{OSi}\equiv$  species. In ethanol, excitation of the solvent adduct  $(\text{CH}_3)_3\text{Sn}-\text{OHC}_2\text{H}_5$  leads to homolytic cleavage and  $\text{I}_2$  formation, which reacts thermally with  $(\text{CH}_3)_3\text{Sn}-\text{OHC}_2\text{H}_5$  to form an  $[(\text{CH}_3)_3\text{Sn}^+, \text{I}_3^-]$  ion pair.

## Introduction

Correlations between the orbital parentage of the reactive state and its dominant mode of reaction, evident in the photochemistry of transition metal complexes,<sup>1–3</sup> have yet to be established with main group complexes. Attempts to

develop these correlations must recognize differences in the thermal chemistry of the complexes. Although some transition metal complexes undergo aquation, most retain a basic coordination geometry in fluid solution, whereas main group metal complexes, specifically tin complexes, are coordination-labile with coordination number and structure functions

\* To whom correspondence should be addressed. E-mail: hgafney@qc1.qc.edu.

- (1) (a) Roundhill, D. M. *Photochemistry and Photophysics of Metal Complexes*; Plenum Press: New York and London, 1994. (b) Balzani, V.; Carassiti, V. *Photochemistry of Coordination Compounds*; Academic Press: New York, 1971. (c) Adamson, A. W.; Waltz, W. I.; Zinato, E.; Watts, D. W.; Fleischauer, P. D.; Lindholm, R. D. *Chem. Rev.* **1968**, 68, 541.
- (2) (a) Kalyanasundram, K. *Photochemistry of Polypyridine and Porphyrin Complexes*; Academic Press: New York, 1992. (b) Kalyanasundram, K. *Coord. Chem. Rev.* **1982**, 46, 159. (c) Balzani, V.; Juris, A.; Barigelletti, F.; Campagna, S.; Belser, P.; Von Zelewsky, A. *Coord. Chem. Rev.* **1988**, 84, 85. (d) Gratzel, M. *Acc. Chem. Res.* **1981**, 14, 376. (e) Novak, A. J. *Photochemical Conversion and Storage of Solar Energy*; Connolly, J. S., Ed.; Academic Press: New York, 1981; p 271. (f) Gratzel, M. *Heterogeneous Photochemical Electron Transfer*; CRC Press: Boca Raton, FL, 1987. (g) Meyer, T. J. *Pure Appl. Chem.* **1986**, 58, 1193. (h) Sutin, N.; Creutz, C. *Pure Appl. Chem.* **1980**, 52, 2717. (i) Balzani, V. *Supramolecular Photochemistry*; D. Riedel: Boston, 1987. (j) Whitten, D. G. *Acc. Chem. Res.* **1984**, 17, 83. (k) Sutin, N.; Creutz, C. *Pure Appl. Chem.* **1980**, 52, 2717. (l) Krause, R. A. *Struct. Bonding* **1987**, 67, 1.

- (3) (a) Peterson, S. H.; Demas, J. N. *J. Am. Chem. Soc.* **1979**, 101, 6571. (b) Peterson, S. H.; Demas, J. N. *J. Am. Chem. Soc.* **1976**, 98, 7880. (c) Giordano, P. J.; Bock, C. R.; Wrighton, M. S.; Interrante, L. V. *J. Am. Chem. Soc.* **1977**, 99, 3187. *J. Am. Chem. Soc.* **1978**, 100, 6960. (d) Casalbani, F.; Mulazzani, Q. G.; Clark, C. D.; Hoffman, M. Z.; Orizondo, P. L.; Perkovic, M. W.; Rillema, D. P. *Inorg. Chem.* **1997**, 36, 2252. (e) Shimidzu, T.; Iyoda, T.; Izaki, K. *J. Phys. Chem.* **1985**, 89, 642. (f) Giordano, P. J.; Bock, C. R.; Wrighton, M. S.; Interrante, L. V. *J. Am. Chem. Soc.* **1977**, 99, 3187. (f) Fergeson, J.; Mau, A.; Sasse, W. H. F. *Chem. Phys. Lett.* **1979**, 68, 21. (g) Lay, P. A.; Sasse, W. H. F. *Inorg. Chem.* **1984**, 23, 4123. (h) Crutchley, R. J.; Kress, N.; Lever, A. B. P. *J. Am. Chem. Soc.* **1983**, 105, 1170. (i) Kirsch-De Mesmaeker, A.; Jacquet, L.; Nasielski, J. *Inorg. Chem.* **1988**, 27, 4451. (j) Nazeeruddin, Md. K.; Kalyanasundaram, K. *Inorg. Chem.* **1989**, 28, 4251. (k) Hosek, W.; Tysoe, S. A.; Baker, A. D.; Streckas, T. C.; Gafney, H. D. *Inorg. Chem.* **1989**, 28, 1228. (l) Hicks, C.; Fan, J.; Rutenberg, I.; Gafney, H. D. Excited State Acid–Base Chemistry: A New Quenching Mechanism. *Coord. Chem. Rev.* **1998**, 171, 71. (m) Dougherty, T.; Hicks, C.; Maletta, A.; Fan, J.; Rutenberg, I.; Gafney, H. D. *J. Am. Chem. Soc.* **1998**, 120, 4226. (n) Hicks, C.; Ye, G.; Levi, C.; Gonzales, M.; Rutenberg, I.; Fan, J.; Helmy, R.; Kassis, A.; Gafney, H. D. *Coord. Chem. Rev.*, in press.

of the solvent in which the complex is dissolved.<sup>4–9</sup> The thermal redox chemistry of the main group metals is also dominated by two-electron processes. One-electron transfer is certainly possible in the high-energy domain of an excited state, but a secondary thermal electron transfer must complement the photoinduced charge transfer to achieve a thermally stable product. Vogler and co-workers note that the reduction of the metal ion and corresponding evolution of N<sub>2</sub> during photolysis of acetonitrile solutions of Sn(N<sub>3</sub>)<sub>6</sub><sup>2–</sup> and Pb(N<sub>3</sub>)<sub>6</sub><sup>2–</sup> correlates with the LMCT character of the spectrally observable lowest excited state but propose a reductive elimination to account for the overall two-electron reduction of the metal.<sup>10</sup>

Our interest in photochemistry of main group complexes, specifically (CH<sub>3</sub>)<sub>3</sub>SnI, stems from its use in changing the refractive index of glass.<sup>11–20</sup> UV photolysis of (CH<sub>3</sub>)<sub>3</sub>SnI adsorbed onto Corning's code 7930 porous Vycor glass (PVG) or porous glassy matrixes derived from the base-catalyzed gelation of tetramethoxysilane, methanol, and water (TMOS/MeOH/H<sub>2</sub>O) increases the refractive index of the exposed regions relative to the bulk glass.<sup>11–20</sup> Subsequent heating drives the unexposed complex from the glass and, at 1200 °C, consolidates the glass, entrapping a photo-generated gradient index pattern in the glass.<sup>20</sup> Previous studies of the photochemistry of (CH<sub>3</sub>)<sub>3</sub>SnI in hydrocarbon solution indicate homolytic cleavage of the (CH<sub>3</sub>)<sub>3</sub>Sn–I following 254 nm excitation with the resulting radicals coupling to form ((CH<sub>3</sub>)<sub>3</sub>Sn)<sub>2</sub> and I<sub>2</sub>.<sup>21–26</sup> However, both

products desorb from the glass during subsequent heating, thereby precluding their involvement in gradient index formation. Furthermore, UV photolysis of (CH<sub>3</sub>)<sub>3</sub>Sn–I adsorbed onto porous Vycor glass yields I<sub>3</sub><sup>–</sup>, suggesting heterolytic cleavage of the (CH<sub>3</sub>)<sub>3</sub>Sn–I bond in the glass matrix.<sup>27</sup> These experiments were undertaken to improve the optical performance of these gradient index structures by establishing the nature of the precursor on the glass surface, identifying the excited state from which the reaction occurs, and detailing the thermal chemistry of the photoproducts generated on the glass.

In hexane, (CH<sub>3</sub>)<sub>3</sub>SnI exists as a discrete, four-coordinate tetrahedron, but adsorbed onto porous glass and in ethanol, the complex exists as a five-coordinate adduct with the oxygen of the surface silanol, or the alcohol, occupying the fifth coordination site. Formation of the five-coordinate adduct causes only slight shifts in the transition energy, and the photochemical reaction continues to occur from the same LMCT state in each medium. However, the products obtained in the different media differ with radical and ionic products obtained in the polar media.<sup>27</sup> A model consistent with the data attributes the formation of ionic products in alcohol to a secondary thermal reaction between I<sub>2</sub> and the five-coordinate alcohol adduct, whereas the ionic products formed on porous glass arise from the thermalization of the radical photoproducts via a subsequent electron transfer.

## Experimental Section

**Materials.** Trimethyltin iodide (CH<sub>3</sub>)<sub>3</sub>SnI (Organometallic, Inc., 99%), hexamethylditin (CH<sub>3</sub>)<sub>6</sub>Sn<sub>2</sub> (Organometallic, Inc., 98.5%), spectroscopic grade *n*-hexane (Aldrich, 98.5%), ethanol (Aldrich, >99%), and *n*-hexanol (Aldrich, >99%) were used as received. Polished 25.4 mm × 25.4 mm × 2.0 mm plates of code 7930 porous Vycor glass (Corning, Inc.) containing a random array of interconnected 10 ± 1 nm diameter pores were extracted with boiling water in a Soxhlet extractor for ≥24 h, dried under reduced pressure (*p* ≤ 10<sup>–3</sup> Torr) at 40 °C, and then calcined at 650 °C for ≥72 h. The calcined samples were stored at this temperature until needed, at which point, a sample was transferred to a vacuum desiccator and cooled to room temperature under vacuum (*p* ≤ 10<sup>–3</sup> Torr).

**Impregnation.** Impregnation was by previously described solution adsorption procedures.<sup>28–30</sup> Calcined, weighed samples of porous Vycor glass (PVG) were immersed in 50.0 mL of an *n*-hexane solution 10<sup>–1</sup>–10<sup>–4</sup> M in (CH<sub>3</sub>)<sub>3</sub>SnI. The number of moles of (CH<sub>3</sub>)<sub>3</sub>SnI adsorbed, which ranged from 10<sup>–7</sup> to 10<sup>–4</sup> mol/g of PVG, was calculated from the decrease in absorption due to (CH<sub>3</sub>)<sub>3</sub>SnI in the surrounding solution at 230 nm ( $\epsilon = 3.45 \times 10^3 \text{ M}^{-1} \text{ cm}^{-1}$ ).<sup>28–30</sup> The impregnated samples were then placed in a desiccator at room temperature and maintained at ≤10<sup>–3</sup> Torr for at least 1 h to remove the hexane incorporated during impregnation.<sup>31</sup>

**Photochemical Procedures.** Hexane and ethanol solutions of (CH<sub>3</sub>)<sub>3</sub>SnI were contained in previously described 1 cm quartz

- (4) (a) Van der Berghe, E. V.; Van der Kelen, G. P. *J. Organomet. Chem.* **1969**, *11*, 479. (b) Van der Berghe, E. V.; Van der Kelen, G. P. *J. Organomet. Chem.* **1969**, *16*, 497.
- (5) Matwiyoff, N. A.; Drago, R. S. *Inorg. Chem.* **1964**, *4*, 337.
- (6) (a) Bolles, T. F.; Drago, R. S. *J. Am. Chem. Soc.* **1965**, *87*, 5015. (b) Bolles, T. F.; Drago, R. S. *J. Am. Chem. Soc.* **1966**, *88*, 392, 5730.
- (7) Thomas, A. B.; Rochow, E. G. *J. Inorg. Nucl. Chem.* **1967**, *4*, 205.
- (8) Cotton F. A.; Wilkinson, G. *Advanced Inorganic Chemistry*, 5th ed.; Wiley-Interscience: New York, 1988; p 292.
- (9) Sawyer, A. K. *Organotin Compound*; Marcel Dekker: New York, 1971; Vol. 1, p 110.
- (10) Vogler, A.; Quett, C.; Paukner, A.; Kunkely, H. *J. Am. Chem. Soc.* **1986**, *108*, 8263.
- (11) Borrelli, N. F.; Morse, D. L.; Schreurs, J. W. H. *J. Appl. Phys.* **1983**, *54* (6), 3344.
- (12) Borrelli, N. F.; Morse, D. L. *Appl. Phys. Lett.* **1983**, *43* (11), 993.
- (13) Gafney, H. D. *J. Imaging Sci.* **1989**, *33* (2), 37.
- (14) Gafney, H. D. A Photochemical Approach to Integrated Optics. In *Chemistry in Industry*; Perry, D., Ed.; American Chemical Society: Plenum Press: New York, 1997; p 189.
- (15) Gafney, H. D. *J. Macromol. Sci., Chem.* **1991**, *A27* (9–11), 1187.
- (16) Mendoza, E. A.; Sunil, D.; Wolkow, E.; Sunil, D.; Wong, P.; Sokolov, J.; Rafailovich, M. H.; den Boer, M.; Gafney, H. D. *Langmuir* **1991**, *7*, 3046.
- (17) Mendoza, E. A.; Wolkow, E.; Rafailovich, M. H.; Sokolov, J.; Gafney, H. D.; Hansen, A. *Mater. Res. Soc. Symp. Proc.* **1990**, *168*, 381.
- (18) Sunil, D.; Rafailovich, M. H.; Sokolov, J.; Gafney, H. D.; Hansen, A. *Mater. Res. Soc. Symp. Proc.* **1990**, *168*, 387.
- (19) Mendoza, E. A.; Wolkow, E.; Rafailovich, M. H.; Sokolov, J.; Gafney, H. D.; Sunil, D.; Long, G. G.; Jamian, P. R. *Appl. Phys. Lett.* **1990**, *57*, 209.
- (20) Mendoza, E. A. Ph.D. Thesis, The City University of New York, 1992.
- (21) Wang, W. L. *Inorg. Chem.* **1967**, *6*, 1061.
- (22) Borrell, P.; Platt, A. E. *J. Chem. Soc., Faraday Trans.* **1970**, *66*, 2279, 2285.
- (23) DeRyck, P. H.; Verdonck, L.; Van der Kelen, G. P. *Int. J. Chem. Kinet.* **1985**, *17*, 95.
- (24) DeRyck, P. H.; Verdonck, L.; Hostes, S.; Van der Kelen, G. P. *Bull. Soc. Chim. Belg.* **1985**, *94*, 621.
- (25) DeRyck, P. H.; Hostes, S.; Van der Kelen, G. P. *Bull. Soc. Chim. Belg.* **1985**, *95*, 217.

- (26) (a) Fuluzumi, S.; Kochi, J. K. *J. Phys. Chem.* **1980**, *84*, 617. (b) Fuluzumi, S.; Kochi, J. K. *J. Org. Chem.* **1980**, *42*, 2654.
- (27) Mendoza, E. A.; Gafney, H. D. *Inorg. Chem.* **1990**, *29*, 4853.
- (28) Shi, W.; Gafney, H. D. *J. Phys. Chem.* **1988**, *92*, 2329.
- (29) Wolfgang, S.; Gafney, H. D. *J. Phys. Chem.* **1983**, *87*, 5395.
- (30) Darsillo, M. S.; Paquett, M. S.; Gafney, H. D. *J. Am. Chem. Soc.* **1987**, *109*, 3275.
- (31) Simon, R. C.; Mendoza, E. A.; Gafney, H. D. *Inorg. Chem.* **1988**, *27*, 2733.

cells<sup>30,31</sup> and irradiated in a Rayonet model RMR-500 photochemical reactor (Southern New England Ultraviolet Company) equipped with 254 nm bulbs. Most photolyses were carried out with air-saturated solutions because deaeration by helium bubbling or degassing by freeze-pump-thaw cycles had no measurable effect on the quantum yield of (CH<sub>3</sub>)<sub>3</sub>SnI disappearance,  $\Phi_{\text{dis}}$ . The photon flux, typically  $8.1 \times 10^{15}$  quantum/s, was determined by ferrioxalate actinometry,<sup>32</sup> and the rates of (CH<sub>3</sub>)<sub>3</sub>SnI disappearance and photoproduct appearance were calculated from UV-visible spectra recorded periodically during photolysis.

Pieces of PVG impregnated with (CH<sub>3</sub>)<sub>3</sub>SnI were rigidly mounted with a Teflon holder in previously described rectangular quartz cells<sup>30,31</sup> and evacuated to a pressure of  $\leq 10^{-3}$  Torr. All samples were irradiated with 254 nm light either under vacuum ( $\leq 10^{-3}$  Torr) or under helium (1 atm) in the Rayonet reactor. The photon flux incident onto the glass sample, typically  $2.7 \times 10^{14}$  quantum  $\text{cm}^{-2} \text{s}^{-1}$ , was calculated from the flux incident onto a ferrioxalate solution contained in an identical quartz cell.<sup>30,31</sup> To minimize uncertainties arising from subtle differences in the distribution of the adsorbate across the  $2.0 \pm 0.1$  mm thickness of the glass samples, kinetic data were recorded on individual pieces cut from a single sample or on a group of samples impregnated together under identical conditions.

UV-visible spectra of the adsorbed complex, designated (CH<sub>3</sub>)<sub>3</sub>-SnI(ads), and the changes occurring during photolysis were recorded as difference spectra relative to that of the untreated glass. The rate of the photochemical reaction was determined by monitoring the rate of disappearance of (CH<sub>3</sub>)<sub>3</sub>SnI(ads) and the rates of appearance of I<sub>2</sub> and/or I<sub>3</sub><sup>-</sup>. Absolute quantum yields were not accessible because of competitive absorption by the glass, 50% transmittance at 297 nm. Instead, estimates of the quantum yields were calculated from the rates of appearance of these species and the average absorbance of (CH<sub>3</sub>)<sub>3</sub>SnI(ads) at 254 nm.

**Physical Measurements.** UV-visible spectra were recorded on an AVIV UV-vis-NIR spectrophotometer. Diffuse reflectance FTIR (DRIFT) spectra of crushed (320 mesh) impregnated PVG samples, diluted 1:30 with KBr, were recorded on a Nicolet Analytical Instruments model 20/5DX FTIR spectrometer.<sup>33</sup> Raman spectra were recorded on a previously described spectrometer using 514.5 nm excitation.<sup>34</sup> Cyclic voltammograms of ethanol solutions of (CH<sub>3</sub>)<sub>3</sub>SnI, 0.1 M in tetramethylammonium tetrafluoroborate, were recorded at scan rates of 20–500 mV/s with previously described equipment using a glassy carbon electrode (Fischer Scientific, no. 13-620-274), a Ag/AgCl combination reference electrode (Orion model 9512), and a Pt wire auxiliary electrode.<sup>35</sup> Mossbauer spectra were recorded on a previously described spectrometer<sup>36</sup> in the constant acceleration mode and calibrated with a 25  $\mu\text{m}$  thick  $\alpha$ -Fe standard ( $\geq 99\%$ , Amersham). Transmission spectra were recorded either at room temperature or at 15 K using a Janis Research low-temperature refrigerator and were fit with Lorentzian functions using the least-squares test.<sup>36</sup> Secondary ion mass spectra (SIMS) were recorded on an Atomika model 3000-30 ion microprobe. Cross-sectional distributions of the adsorbed complex were measured by impinging an Ar<sup>+</sup> beam at a voltage of 6.0 kV and a scan width of 0.5 mm onto the sample at an angle

of 30° relative to its surface. The amount of tin displaced from the sample as a function of depth was measured relative to Si as a reference.

## Results

The electronic spectrum of (CH<sub>3</sub>)<sub>3</sub>SnI consists of a lower-energy UV absorption whose maximum and intensity reflect the medium in which it is recorded and unresolved higher-energy absorptions occurring at  $< 200$  nm.<sup>18</sup> In hexane, the lower-energy transition occurs at 234 nm ( $\epsilon = 3.45 \times 10^3 \text{ M}^{-1} \text{ cm}^{-1}$ ) and shifts to shorter wavelength as solvent polarity increases. The largest shift occurs in solvents possessing oxygen donor atoms shifting to 226 nm ( $\epsilon = 5.27 \times 10^3 \text{ M}^{-1} \text{ cm}^{-1}$ ) in acetonitrile, 221 nm ( $\epsilon = 8.85 \times 10^3 \text{ M}^{-1} \text{ cm}^{-1}$ ) in hexanol, and 218 nm ( $\epsilon = 1.54 \times 10^4 \text{ M}^{-1} \text{ cm}^{-1}$ ) in ethanol.

Adsorbed onto PVG, difference spectra reveal higher-energy absorptions at  $< 200$  nm and a resolved absorption with a maximum at 230 nm. The intensity of the latter band increases in proportion to the number of moles of (CH<sub>3</sub>)<sub>3</sub>-SnI adsorbed per gram of glass, but the wavelength maximum is independent of the amount adsorbed, suggesting that aggregation of the adsorbate is minimal. Electronic spectra recorded at different locations on the same sample are identical, and SIMS analyses of the impregnated samples yield a uniform distribution of tin to a depth of at least 400 nm. Assuming a uniform cross-sectional distribution of (CH<sub>3</sub>)<sub>3</sub>SnI(ads) and taking  $183 \pm 15 \text{ m}^2/\text{g}$  as the surface area of the glass<sup>28,30</sup> and  $0.18 \text{ nm}^2$  as the area covered by the individual molecules, the loadings examined in these experiments,  $10^{-7}$ – $10^{-4}$  mol/g, correspond to fractional surface coverages of  $\leq 10\%$ .

The silanol bands of calcined PVG appear as a sharp band at  $3744 \text{ cm}^{-1}$  and as a lower-intensity shoulder at ca.  $3650 \text{ cm}^{-1}$  that are assigned to the free and associated hydrogen-bonded silanol groups, respectively.<sup>37,38</sup> Adsorption of (CH<sub>3</sub>)<sub>3</sub>-SnI reduces the intensity of these bands (Figure 1) and leads to the appearance of bands at  $2993$  and  $2917 \text{ cm}^{-1}$  and an intense, broad band centered at  $3550 \text{ cm}^{-1}$ . Trace amounts of water are present in the calcined glass, but the latter band does not arise from water formation or its displacement from the glass.<sup>30,31</sup> The spectral changes are proportional to the amount of (CH<sub>3</sub>)<sub>3</sub>SnI adsorbed and are reversible under vacuum at room temperature with recovery of the desorbed complex. The absence of desorbed water in the recovered material confirms that the broad absorption at  $3550 \text{ cm}^{-1}$  arises from the reversible adsorption of (CH<sub>3</sub>)<sub>3</sub>SnI.

The <sup>119</sup>Sn Mossbauer spectrum of (CH<sub>3</sub>)<sub>3</sub>SnI adsorbed onto PVG,  $1.7 \times 10^{-5}$  mol/g, shows a well-resolved quadrupole doublet with an isomer shift of  $1.06 \text{ mm/s}$  relative to SnO<sub>2</sub> and a quadrupole splitting of  $3.14 \text{ mm/s}$ . The isomer shift and quadrupole splittings are independent of loading, albeit limited to loadings of  $5 \times 10^{-6}$  and  $2 \times 10^{-5}$  mol/g.

In solution and adsorbed onto the glass, (CH<sub>3</sub>)<sub>3</sub>SnI reacts immediately on exposure to UV light. The quantum yield

(32) Calvert, J. G.; Pitts, J. N. *Photochemistry*; Wiley: New York, 1966; pp 332–334.

(33) Dieter, T.; Gafney, H. D. *Inorg. Chem.* **1988**, *27*, 1730.

(34) Knorrs, C.; Gafney, H. D.; Baker, A. D.; Braunstein, C. H.; Streckas, T. C. *J. Raman Spectrosc.* **1983**, *14*, 32.

(35) Braunstein, C. H.; Baker, A. D.; Streckas, T. C.; Gafney, H. D. *Inorg. Chem.* **1984**, *23*, 857.

(36) Sunil, D.; Rafailovich, M. H.; Sokolov, J.; Kotyuhanski, B.; Gafney, H. D.; Wilkins, B.; Hanson, A. L. *J. Appl. Phys.* **1993**, *74*, 3768.

(37) (a) Hair, M. L.; Chapman, I. D. *J. Am. Ceram. Soc.* **1966**, *49*, 651.

(b) Hair, M. L.; Chapman, I. D. *Trans. Faraday Soc.* **1965**, *61*, 1507.

(38) (a) Cant, N. W.; Little, L. H. *Can. J. Chem.* **1964**, *42*, 802. (b) Cant, N. W.; Little, L. H. *Can. J. Chem.* **1965**, *43*, 1252.

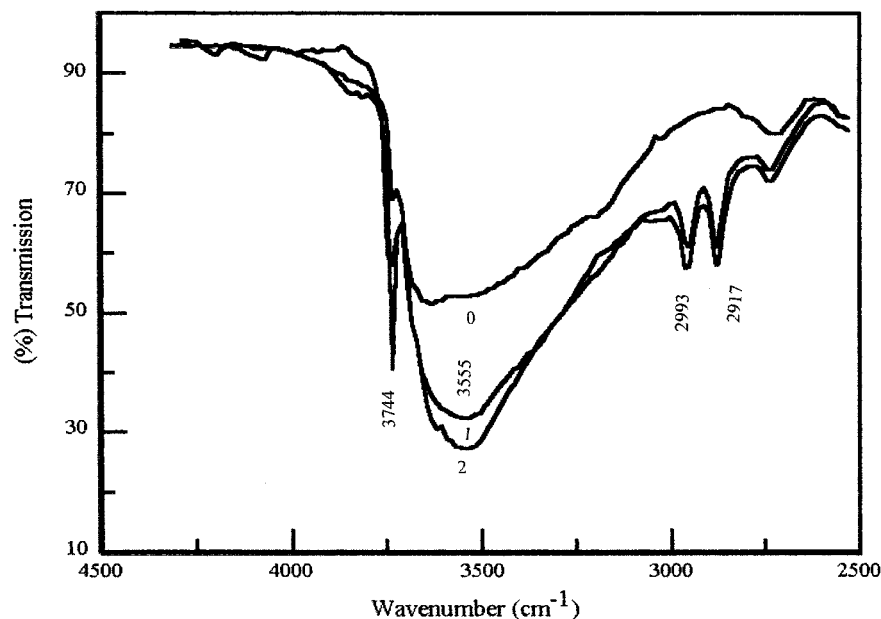


**Figure 1.** Diffuse reflectance FTIR spectra of porous Vycor glass after exposure to  $10^{-6}$  Torr of  $(\text{CH}_3)_3\text{SnI}$ . Numbers refer to spectra recorded immediately (0) and 1 and 2 min after exposure. Little further change occurs in the spectrum after 2 min.

of  $(\text{CH}_3)_3\text{SnI}$  disappearance in each medium is independent of  $(\text{CH}_3)_3\text{SnI}$  concentration or loading, independent of  $\text{O}_2$  concentration, and very dependent on excitation wavelength. In hexane, the quantum yield of  $(\text{CH}_3)_3\text{SnI}$  disappearance,  $0.32 \pm 0.05$  with 254 nm excitation, declines to  $0.11 \pm 0.06$  with 310 nm excitation and is  $\leq 10^{-3}$  with 350 nm excitation. Equivalent spectral changes occur with 254 or 310 nm excitation; a decline in  $(\text{CH}_3)_3\text{SnI}$  absorbance at 234 nm is accompanied by an immediate appearance of bands at 290, 365, and 520 nm. A higher-energy absorption also appears as a shoulder at 210 nm and increases in intensity during photolysis.<sup>27</sup> The 520 nm absorption is identical to that of  $\text{I}_2$  dissolved in hexane and confirms  $\text{I}_2$  formation, while the shoulder at 210 nm is equivalent to that of  $\text{Sn}_2(\text{CH}_3)_6$  in hexane and confirms its formation. The peaks at 290 and 365 nm are assigned to the formation of  $\text{I}_3^-$  because the maxima are identical to those observed on shaking a hexane solution of  $\text{I}_2$  with excess KI and agree with the reported maxima of  $\text{I}_3^-$ .<sup>39</sup> Despite the intensities of the  $\text{I}_3^-$  bands, the amount of  $\text{I}_3^-$  formed, calculated from the observed changes in absorbance at 290 and 365 nm ( $\epsilon_{290} = 4.81 \times 10^4 \text{ M}^{-1} \text{ cm}^{-1}$ ;  $\epsilon_{365} = 2.70 \times 10^4 \text{ M}^{-1} \text{ cm}^{-1}$ ), never exceeds 2% of the amount of  $\text{I}_2$  formed. Consistent with previous studies,<sup>26</sup> stoichiometric measurements yield  $0.50 \pm 0.05$  mol of  $\text{I}_2$  formed per mole of  $(\text{CH}_3)_3\text{SnI}$  consumed, and adding the radical scavenger isoamyl nitrite,<sup>40</sup>  $10^{-4}$  M, does not affect the quantum efficiency of  $(\text{CH}_3)_3\text{SnI}$  disappearance but reduces the quantum efficiencies of  $\text{I}_2$  and  $\text{Sn}_2(\text{CH}_3)_6$  formation from  $0.18 \pm 0.04$  to  $0.05 \pm 0.01$ .

Although corrected for consumption of  $(\text{CH}_3)_3\text{SnI}$ , the quantum yield of  $(\text{CH}_3)_3\text{SnI}$  disappearance in hexane declines with increasing photolysis. An increase in absorption at 234

nm indicates that the decline in yield is due to the photo-products  $\text{I}_2$  and  $\text{Sn}_2(\text{CH}_3)_6$  reacting to re-form  $(\text{CH}_3)_3\text{SnI}$ . Separate experiments with  $\text{I}_2$  and  $\text{Sn}_2(\text{CH}_3)_6$  in hexane establish that the reaction exhibits first-order dependencies on the concentrations of  $(\text{CH}_3)_3\text{Sn-Sn}(\text{CH}_3)_3$  and  $\text{I}_2$  and occurs with a rate constant of  $(2.26 \pm 0.01) \times 10^2 \text{ M}^{-1} \text{ s}^{-1}$  at 25 °C.

To gain insights into the thermal and photochemical behavior of  $(\text{CH}_3)_3\text{SnI}$  on the hydroxylated surface of PVG, its behavior was examined in alcohols. The electronic spectrum of  $(\text{CH}_3)_3\text{SnI}$  in alcohol is very similar to that in hexane except that the lower-energy transition shifts to 218 nm in ethanol and to 221 nm in hexanol and more than doubles in intensity in both alcohols. The spectral changes are proportional to the amount of alcohol, and titration of a  $7.37 \times 10^{-4}$  M hexane solution of  $(\text{CH}_3)_3\text{SnI}$  with hexanol occurs with retention of an isosbestic point at 237 nm. Job's plots constructed from the change in absorbance at 211 nm as a function of the mole fraction of hexanol and  $(\text{CH}_3)_3\text{SnI}$  exhibit a maximum at 0.5, indicating the formation of a 1:1  $(\text{CH}_3)_3\text{SnI}$ /hexanol adduct. Equivalent changes, but with a maximum at 218 nm, indicate that a similar adduct forms with ethanol. Formation of the ethanol adduct shifts the ethanol O-H vibration from 3635 to 3350  $\text{cm}^{-1}$  in the 1:1  $(\text{CH}_3)_3\text{SnI}/\text{C}_2\text{H}_5\text{OH}$  adduct. The spectral changes fail to convey the magnitude of the effect of adduct formation on the Sn-I bond. Electronic spectra of a  $2.0 \times 10^{-4}$  M hexane solution of  $(\text{CH}_3)_3\text{SnI}$  to which  $\text{I}_2$  is added give no indication of a reaction. Adding  $\text{I}_2$  to an ethanol solution  $1.0 \times 10^{-4}$  M in  $(\text{CH}_3)_3\text{SnI}$ , however, results in the immediate appearance of bands at 362 and 292 nm. The latter absorptions are identical to those of  $\text{I}_3^-$ ,<sup>39</sup> and scanning voltammetry and titration with  $\text{Ag}(\text{NO}_3)$  confirm iodide ion formation. Job's plots of the absorbance changes vs the mole fraction of  $\text{I}_2$  exhibit maxima at a mole fraction of 0.5, confirming the

(39) (a) Mitchell, T. N.; el-Behairy, M. *Helv. Chim. Acta* **1981**, *64* (3), 628. (b) Awtrey, A. D.; Connick, R. E. *J. Am. Chem. Soc.* **1951**, *73*, 1842.

(40) Armistead, C. G.; Hockey, J. A. *Trans. Faraday Soc.* **1967**, *63*, 2549.

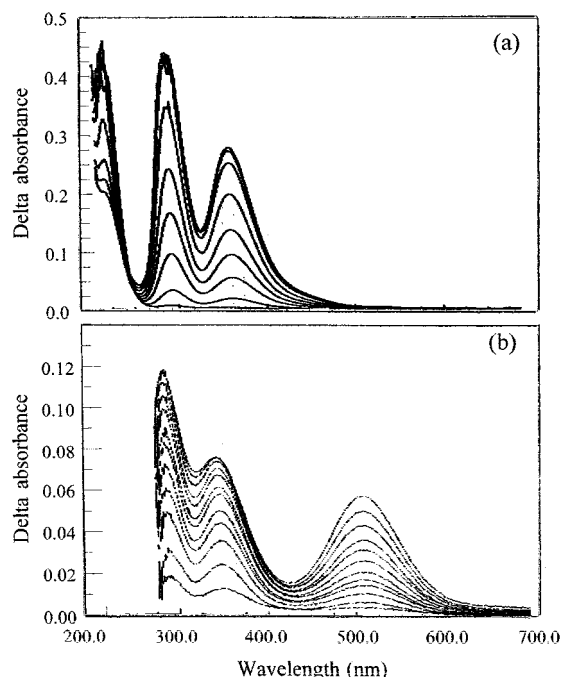


**Figure 2.** (a) UV-visible spectra recorded during 254 nm photolysis of a  $3.8 \times 10^{-3}$  M solution of  $(\text{CH}_3)_3\text{SnI}$  in ethanol. The absorbance at 212 nm declines, while those at longer wavelengths increase during photolysis. (b) UV-visible spectra recorded relative to untreated PVG during 254 nm photolysis of a sample of PVG containing  $1.6 \times 10^{-6}$  mol of  $(\text{CH}_3)_3\text{SnI/g}$ . The absorbance of each band increases during photolysis.

formation of a 1:1  $[(\text{CH}_3)_3\text{Sn}^+, \text{I}_3^-]$  ion pair. There is no evidence of asymmetry in the plots, thereby negating the formation of higher-order polyiodides.<sup>34</sup>

Unlike in hexane, where the 210 and 450 nm bands signal immediate  $(\text{CH}_3)_6\text{Sn}_2$  and  $\text{I}_2$  formation, a 254 nm photolysis of  $(\text{CH}_3)_3\text{SnI-OHC}_2\text{H}_5$  in ethanol causes an immediate appearance of bands at 290 and 360 nm (Figure 2a). The latter absorptions are assigned to  $\text{I}_3^-$ <sup>27</sup> because the ion exhibits absorptions at 290 nm ( $\epsilon = 4.02 \times 10^4 \text{ M}^{-1} \text{ cm}^{-1}$ ) and 361 nm ( $\epsilon = 2.62 \times 10^4 \text{ M}^{-1} \text{ cm}^{-1}$ ) in ethanol, and the relative band intensities are within experimental error of the ratio of the molar extinction coefficients. An absorption at 450 nm attributable to  $\text{I}_2$  appears as a shoulder on the 360 nm absorption but only after ca. 50% consumption of the  $(\text{CH}_3)_3\text{SnI}$ . Raman spectra recorded during photolysis show that the decline in the intensity of the  $167 \text{ cm}^{-1}$  Sn-I vibration is not accompanied by a concurrent increase in the  $186 \text{ cm}^{-1}$  Sn-Sn vibration of  $(\text{CH}_3)_6\text{Sn}_2$ . Mossbauer spectra of the photolyte cooled to 15 K exhibit a weak, broad absorption with a low signal-to-noise ratio. Attempts to resolve the absorption with Lorentzian functions derived from the isomer shifts and quadrupole splittings of  $(\text{CH}_3)_6\text{Sn}_2$  and possible alcoholate products, such as  $(\text{CH}_3)_3\text{SnOC}_2\text{H}_5$ , however, failed to reproduce the broadness of the observed signal and achieve a satisfactory fit.<sup>41-44</sup>

As in hexane, the quantum yield of  $(\text{CH}_3)_3\text{SnI}$  disappearance in ethanol is independent of  $\text{O}_2$  and  $(\text{CH}_3)_3\text{SnI}$  concentration and declines from  $0.61 \pm 0.06$  with 254 nm excitation to  $\leq 0.01$  and  $\leq 0.001$  with 310 and 350 nm excitation, respectively. The quantum yield of  $\text{I}_3^-$  formation,  $0.23 \pm 0.04$ , with 254 nm excitation, is independent of added  $\text{I}_2$ , implying that  $\text{I}_3^-$  is not derived from the photolysis of  $[(\text{CH}_3)_3\text{SnOHC}_2\text{H}_5^+, \text{I}_3^-]$  ion pairs. Rather, the consistent appearance of  $\text{I}_2$ , but at a slower rate than the appearance of  $\text{I}_3^-$ , suggests that the photochemical reaction generates  $\text{I}_2$ , but it reacts thermally with the  $(\text{CH}_3)_3\text{SnI-OHC}_2\text{H}_5$  adduct to form the  $[(\text{CH}_3)_3\text{SnOHC}_2\text{H}_5^+, \text{I}_3^-]$  ion pair. Assuming quantitative formation of the  $[(\text{CH}_3)_3\text{SnOHC}_2\text{H}_5^+, \text{I}_3^-]$  ion pair, i.e., each  $\text{I}_2$  formed goes on to form an ion pair, the expected yield of  $\text{I}_3^-$ ,  $0.31 \pm 0.3$ , is only slightly larger than the actual quantum yield of  $\text{I}_3^-$  formation,  $0.23 \pm 0.04$ .

PVG possesses a hydroxylated surface,<sup>37,38</sup> and although the strong absorbance of the glass masks part of the UV, difference spectra reveal changes similar to those found in ethanol. A 254 nm photolysis of a PVG sample containing  $1.6 \times 10^{-6}$  mol/g  $(\text{CH}_3)_3\text{SnI}$ , corresponding to a surface coverage of ca. 0.1%, leads to the immediate appearance of three bands at 295, 365, and 508 nm (Figure 2b). The 508 nm band agrees with the absorption spectrum of  $\text{I}_2$  adsorbed onto PVG ( $\epsilon_{508} = 7.8 \times 10^4 \text{ g/mol}$ ) and establishes  $\text{I}_2$  formation, while the bands at 295 and 365 nm agree with the spectrum of  $\text{I}_3^-$  adsorbed onto PVG ( $\epsilon_{290} = 4.1 \times 10^6 \text{ g/mol}$ ,  $\epsilon_{365} = 2.7 \times 10^6 \text{ g/mol}$ ) and establish its formation on the glass.  $\text{I}_3^-$  is not a consequence of the formation of  $[(\text{CH}_3)_3\text{Sn}^+, \text{I}_3^-]$  ion pairs on the glass surface because UV-visible spectra give no indication of  $\text{I}_3^-$  formation when a glass containing  $1.6 \times 10^{-6}$  mol of  $(\text{CH}_3)_3\text{SnI(ads)/g}$  is exposed to a hexane solution saturated with  $\text{I}_2$ . Nor does  $\text{I}_2$  formation on the glass arise from the secondary photolysis of  $\text{I}_3^-$ .<sup>17</sup> Extrapolating the number of moles of  $\text{I}_2$  and  $\text{I}_3^-$  formed back to zero irradiation time gives no indication of an induction period preceding the formation of either species. Both species appear to be formed concurrently, and in all experiments, more  $\text{I}_2$  is formed than  $\text{I}_3^-$ , but the rate of formation of  $\text{I}_2$  is much slower than the rate of photodecomposition of  $(\text{CH}_3)_3\text{SnI(ads)}$ . Nonetheless, on prolonged photolysis, all  $\text{I}_3^-$  converts to  $\text{I}_2$ , and the number of moles of  $\text{I}_2$  formed is exactly half the number of moles of  $(\text{CH}_3)_3\text{SnI}$  adsorbed on PVG, indicating no other iodine-containing product is produced.

Mossbauer spectra of the photolyzed sample (Figure 3) consist of an absorption that resolves into two components. One component corresponds to a singlet with a chemical shift of 1.16 mm/s relative to  $\text{SnO}_2$ , while the other corresponds to a doublet with an isomer shift of 1.12 mm/s and a quadrupole splitting of 3.05 mm/s.

## Discussion

The methyl localized  $\sigma \rightarrow \sigma^*$  and interligand Sn-CH<sub>3</sub> charge-transfer transitions are calculated to occur at  $\leq 200$  nm,<sup>10</sup> and because of their energies, they appear to play little or no role in these experiments where the excitation is limited to wavelengths of  $\geq 254$  nm. The lower-energy transition

(41) Abras, A.; Berry, F. J.; Holden, J. G.; Filgueiras, C. A. L. *Inorg. Chim. Acta* **1983**, *74*, 135.

(42) Debye, N. W. E.; Rosenberg, E.; Zuckerman, J. J. *J. Am. Chem. Soc.* **1968**, *90*, 3234.

(43) Bancroft, G. M.; Platt, R. H. *Adv. Inorg. Chem. Radiochem.* **1972**, *15*, 59.

(44) Cordey-Hays, M.; Peacock, R. D.; Vucelic, M. J. *Inorg. Nucl. Chem.* **1967**, *29*, 1177.

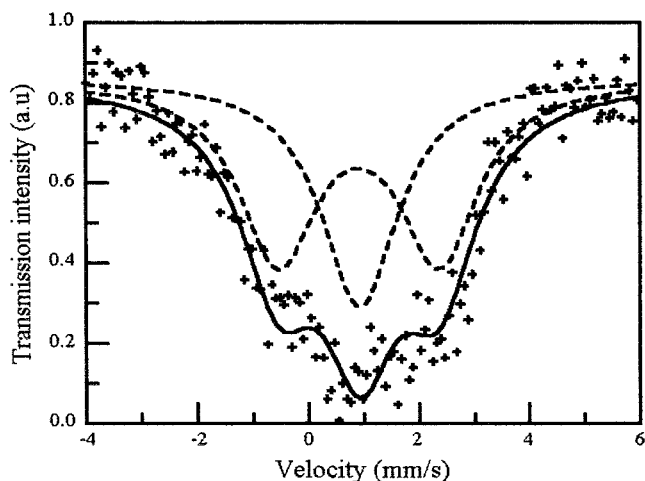


**Figure 3.** Tin-119 Mossbauer spectrum of the photoproducts derived from a 254 nm photolysis of  $(\text{CH}_3)_3\text{SnI}$  adsorbed onto PVG (line represents the computer fit of the data).

depends on the medium shifting from 234 nm to shorter wavelengths in alcohol and adsorbed onto porous glass. Nevertheless, in all the media examined, including that adsorbed onto porous glasses, the transition maximum shifts to lower energy with increasing atomic number of the halide establishing ligand to metal charge transfer (LMCT) character.<sup>1,10</sup> Consistent with the LMCT character, recent CASSCF/MS-CASPT2 calculations assign the 234 nm band to a  $5p(\text{I}) \rightarrow \sigma^*_{\text{Sn-I}}$  transition.<sup>45</sup>

In hexane, the  $(\text{CH}_3)_3\text{SnI}$  species exist as individual tetrahedra and 254 nm light, which excites the molecule on the long-wavelength side of the 234 nm LMCT transition, leads to immediate  $(\text{CH}_3)_3\text{Sn}-\text{Sn}(\text{CH}_3)_3$  and  $\text{I}_2$  formation. The absence of an  $\text{O}_2$  dependence and the decline in the quantum yield of  $(\text{CH}_3)_3\text{SnI}$  disappearance,  $\Phi_{\text{dis}}$ , with increasing excitation wavelength point to a reaction initiating from the LMCT state corresponding to the 234 nm absorption. The stoichiometry of the photoreaction and the reduction in the quantum efficiency of  $(\text{CH}_3)_6\text{Sn}_2$  and  $\text{I}_2$  formation in the presence of isoamyl nitrite establish homolytic cleavage of the  $(\text{CH}_3)_3\text{Sn}-\text{I}$  bond with the resulting radicals coupling to form  $(\text{CH}_3)_3\text{Sn}-\text{Sn}(\text{CH}_3)_3$  and  $\text{I}_2$ .<sup>22-26</sup>

Addition of ethanol or hexanol to hexane solutions of  $(\text{CH}_3)_3\text{SnI}$  results in spectral changes in proportion to the amount of alcohol added, and Job's plots of the data yield a maximum indicative of the formation of a 1:1 adduct. Formation of the adduct is not accompanied by loss of a methyl group or iodine atom or a loss of the alcohol O-H stretch thereby precluding a displacement reaction and formation of an alkoxide. Instead, the ethanol O-H stretch shifts from 3635 to 3350  $\text{cm}^{-1}$  in the presence of  $(\text{CH}_3)_3\text{SnI}$ , suggesting an interaction between the tin atom and alcohol oxygen, which reduces the O-H bond strength.

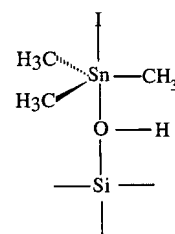
Similar spectral changes when the complex adsorbs onto PVG suggest that adsorption also involves the formation of a surface adduct. The decline in the 3744 and 3650  $\text{cm}^{-1}$

**Table 1.** Mossbauer Parameters of  $(\text{CH}_3)_3\text{SnI}$  in Different Media

	temperature (K)	isomer shift <sup>a</sup> (mm/s)	quadrupole splitting (mm/s)	$\rho(\text{QS})/(\text{IS})$ <sup>b</sup>
bulk sample <sup>41</sup>	78	1.49	3.10	2.08
matrix-isolated <sup>50</sup>	4.2	1.28	2.33	1.82
adsorbed on PVG	15	1.06	3.14	2.96

<sup>a</sup> Relative to  $\text{SnO}_2$ . <sup>b</sup> QS = quadrupole splitting. IS = isomer shift.

silanol bands<sup>37,38</sup> accompanied by the growth of a broad absorption centered at 3550  $\text{cm}^{-1}$  and bands at 2993 and 2917  $\text{cm}^{-1}$  (Figure 1) point to a reaction with the surface silanol groups of the glass. This is corroborated by Mossbauer spectra where the ratio of the quadrupole splitting to isomer shift,  $\rho$ , correlates with the oxidation state and coordination of tin atoms.<sup>50,51</sup> Values of  $\rho$  of  $\leq 2$  are indicative of a tetrahedral complex, whereas values greater than 2 indicate a tin atom with a coordination number of 5 or higher.<sup>46,47</sup> The ratio obtained for the adsorbed complex, 2.96, is clearly within the range expected for five- or six-coordinated tin. Since tin compounds are capable of forming 1:1 and 1:2 adducts, the broadness of the 3550  $\text{cm}^{-1}$  band could be interpreted as the presence of both five- and six-coordinate surface adducts. However, the silanol number of the glass, 4–7  $\text{SiOH}/\text{nm}$ ,<sup>37,38</sup> suggests that the dominant species on the surface is a five-coordinate adduct. Taking an average of 5  $\text{SiOH}/1 \text{ nm}^2$ <sup>49</sup> and assuming these are located at corners and center of a 1 nm  $\times$  1 nm square, the projected area covered by  $(\text{CH}_3)_3\text{SnI}$ , 0.18  $\text{nm}^2$ , indicates that no more than one silanol group would be close enough to form a bond to the tin atom. The value of  $\rho$  for the adsorbed complex  $(\text{CH}_3)_3\text{SnI}(\text{ads})$ , 2.96, also falls within the range, 2.76–3.86 mm/s, found for trigonal bipyramidal tin complexes with axial ligands,<sup>41,44,50</sup> and the quadrupole splitting for the adsorbed complex, 3.14 mm/s, is very close to that of bulk  $(\text{CH}_3)_3\text{SnI}$ , 3.10 mm/s (Table 1), where  $(\text{CH}_3)_3\text{SnI}$  exists in polymeric chains of five-coordinate tin.<sup>51</sup> Since the coordination in the solid state is trigonal bipyramidal with planar  $(\text{CH}_3)_3\text{Sn}$  moieties,<sup>52</sup> the dominant species on the glass surface is taken to be the surface-bound adduct



Analogous to the ethanol adduct  $(\text{CH}_3)_3\text{Sn}-\text{OHC}_2\text{H}_5$ , the tin atom interacts with the lone pair of the silanol oxygen,

(45) Ben Amor, N.; Daniel, C. *Coord. Chem. Rev.* **2001**, submitted; Abstracts of the 14th International Symposium on the Photophysics and Photochemistry of Coordination Compounds, Veszprem, Hungary, 2001, p 66.

(46) Herber, R. H.; Stockler, H. A.; Reichle, W. T. *J. Chem. Phys.* **1985**, *42* (7), 2447.

(47) Eng, G.; Richie, K. L.; May, L. *Inorg. Chim. Acta* **1980**, *43*, 233.

(48) Winkler, W.; Vetter, R. *Hyperfine Interact.* **1990**, *61*, 1185.

(49) Snyder, L. R.; Ward, J. W. *J. Phys. Chem.* **1966**, *70*, 3941.

(50) Goldanskii, V. L.; Herber, R. H. *Chemical Applications of Mossbauer Spectroscopy*; Academic Press: New York, 1968; pp 314–376.

(51) Bukshpan, S.; Pattyn, H. *Chem. Phys. Lett.* **1991**, *177* (3), 269.

(52) Cotton, F. A.; Wilkinson, G. *Advanced Inorganic Chemistry*, 5th ed.; Wiley-Interscience: New York, 1988; p 292.

shifting the silanol bands from 3744 and 3650  $\text{cm}^{-1}$  to 3550  $\text{cm}^{-1}$ . The broadness of the 3550  $\text{cm}^{-1}$  band suggests a range of interactions, which is thought to reflect differences in the local topology and/or the availability of free and associated silanol groups at the individual adsorption sites.<sup>37,38,49,53,54</sup>

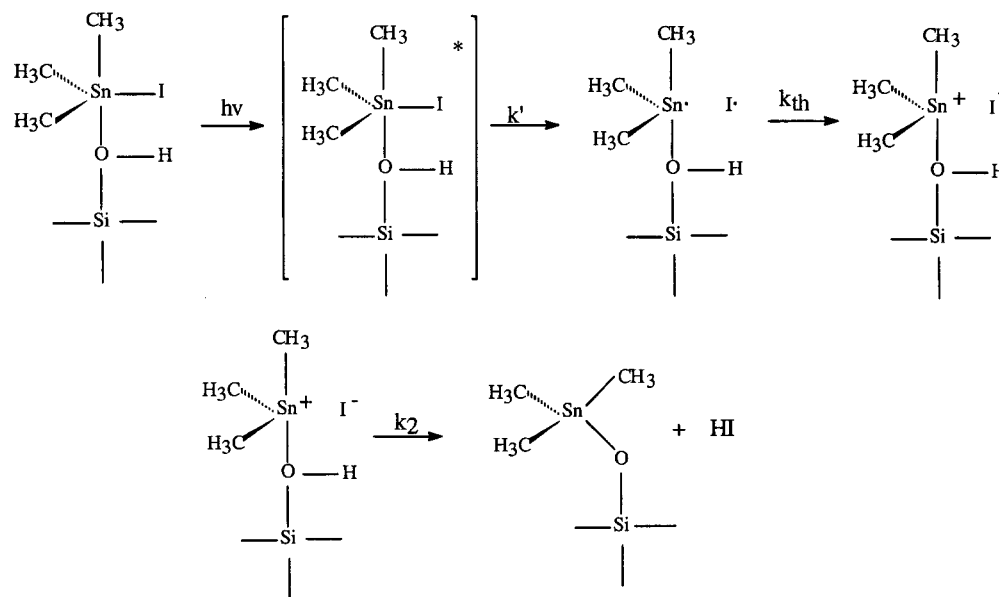
Although similar, the adducts formed in these hydroxylated media exhibit different thermal chemistries. At room temperature, the ethanol adduct reacts immediately with  $\text{I}_2$  to form a 1:1  $[(\text{CH}_3)_3\text{Sn}-\text{OHC}_2\text{H}_5^+, \text{I}_3^-]$  ion pair, whereas no equivalent reaction occurs in PVG. Formation of the  $(\text{CH}_3)_3\text{SnI}$ /ethanol adduct increases the ionic character of the Sn–I bond to a point where  $\text{I}_2$  addition leads to immediate  $\text{I}^-$  dissociation and formation of the 1:1  $[(\text{CH}_3)_3\text{Sn}-\text{OHC}_2\text{H}_5^+, \text{I}_3^-]$  ion pair, or the fluidity of the solution allows better solvation, thereby stabilizing the ionic reaction products. In either case, this thermal reaction affects the outcome of the photochemical reaction in that 254 nm excitation of the  $(\text{CH}_3)_3\text{SnI}-\text{OHC}_2\text{H}_5$  adduct in ethanol leads to the immediate appearance of  $\text{I}_3^-$ . The absence of a dependence on added  $\text{I}_2$  precludes  $\text{I}_3^-$  formation via excitation of an  $[(\text{CH}_3)_3\text{Sn}-\text{OHC}_2\text{H}_5^+, \text{I}_3^-]$  ion pair. Rather, the wavelength dependence of the quantum yield of  $(\text{CH}_3)_3\text{SnI}-\text{OHC}_2\text{H}_5$  disappearance,  $\Phi_{\text{dis}}^{\text{et}}$ , and the absence of an  $\text{O}_2$  dependence point to a reaction occurring from the same LMCT state populated in hexane.  $\text{I}_3^-$  formation led to the suggestion of heterolytic cleavage of the Sn–I bond,<sup>27</sup> but the postulate is not supported by these experiments. In the presence of  $\text{I}_2$ , heterolytic cleavage is expected to produce  $\text{I}_3^-$  with a quantum efficiency,  $\Phi_{\text{I}_3^-}$ , equivalent to the quantum yield of  $(\text{CH}_3)_3\text{SnI}-\text{OHC}_2\text{H}_5$  disappearance,  $\Phi_{\text{dis}}^{\text{et}}$ . Yet, the reaction is independent of  $\text{I}_2$  concentration, and  $\Phi_{\text{I}_3^-}$ ,  $0.23 \pm 0.04$ , is ca. one-third  $\Phi_{\text{dis}}^{\text{et}}$ ,  $0.61 \pm 0.06$ . The appearance of  $\text{I}_2$  as a reaction product after ca. 50% consumption of  $(\text{CH}_3)_3\text{SnI}-\text{OHC}_2\text{H}_5$  points to a different mechanism, where 254 nm excitation of the  $(\text{CH}_3)_3\text{SnI}-\text{OHC}_2\text{H}_5$  adduct continues to result in homolytic cleavage of the Sn–I bond. The resultant iodine atoms couple to form  $\text{I}_2$ , but in ethanol,  $\text{I}_2$  immediately reacts thermally with  $(\text{CH}_3)_3\text{SnI}-\text{OHC}_2\text{H}_5$  to form  $[(\text{CH}_3)_3\text{Sn}-\text{OHC}_2\text{H}_5^+, \text{I}_3^-]$ . Assuming each  $\text{I}_2$  formed reacts quantitatively with the  $(\text{CH}_3)_3\text{SnI}-\text{OHC}_2\text{H}_5$  adduct to form  $[(\text{CH}_3)_3\text{Sn}-\text{OHC}_2\text{H}_5^+, \text{I}_3^-]$ , at least during the initial stages of photolysis,  $\Phi_{\text{I}_2}$ ,  $0.23 \pm 0.04$  in ethanol, implies a quantum yield of  $(\text{CH}_3)_3\text{SnI}-\text{OHC}_2\text{H}_5$  disappearance of  $0.69 \pm 0.12$ , which is within experimental error of the measured value of  $\Phi_{\text{dis}}^{\text{et}}$ ,  $0.61 \pm 0.06$ . As the concentration of  $(\text{CH}_3)_3\text{SnI}-\text{OHC}_2\text{H}_5$  declines, however,  $\text{I}_2$  becomes a detectable reaction product. The appearance of  $\text{I}_2$  on prolonged photolysis points to homolytic cleavage, but the absence of the 186  $\text{cm}^{-1}$  band of  $(\text{CH}_3)_6\text{Sn}_2$  concurrent with the decline in the 167  $\text{cm}^{-1}$  Sn–I vibration of  $(\text{CH}_3)_3\text{SnI}$  precludes coupling of the  $(\text{CH}_3)_3\text{Sn}$  radicals. We return to the fate of these species below.

In contrast to only  $\text{I}_3^-$  formation in ethanol, a 254 nm photolysis of  $(\text{CH}_3)_3\text{Sn}-\text{OHSi}$  yields both  $\text{I}_3^-$  and  $\text{I}_2$  (Figure 2b), with  $\text{I}_2$  being the dominant product.  $\text{I}_3^-$  formation does not arise from a thermal reaction between  $\text{I}_2$  and  $(\text{CH}_3)_3\text{SnI}-\text{OHSi}$  because that reaction does not occur on the glass surface. Instead, the absence of a preceding induction period

suggests that both species are formed concurrently. Resolution of the Mossbauer spectrum of the photolyzed samples (Figure 3) reveals a singlet with an isomer shift of 1.16 mm/s that agrees with the reported isomer shift of hexamethylditin,  $(\text{CH}_3)_6\text{Sn}_2$ , and indicates its formation. The doublet with an isomer shift of 1.12 mm/s and a quadrupole splitting of 3.05 mm/s is assigned to  $(\text{CH}_3)_3\text{Sn}-\text{O}-\text{Si}\equiv$  because the isomer shift and quadrupole splitting of this component are within the range of those reported for trialkyltin alkoxides.<sup>41,44,50,51</sup> We suspect that a similar product forms in ethanol, which we tentatively assign to  $(\text{CH}_3)_3\text{Sn}-\text{OC}_2\text{H}_5$ , but the inability to fit specifically the broadness of the Mossbauer resonance even at 15 K suggests a mixture of five- and six-coordinate adducts, such as  $(\text{CH}_3)_3\text{Sn}-\text{OC}_2\text{H}_5$  and  $(\text{CH}_3)_3\text{Sn}-\text{OC}_2\text{H}_5-(\text{OHC}_2\text{H}_5)$  in ethanol.<sup>50</sup>

Despite the structural difference, there is no spectral evidence of a new state(s) or evidence that the reaction initiates from a different excited state in the hydrocarbon or hydroxylated media. In each medium, the  $\text{O}_2$  and wavelength dependencies of  $\Phi_{\text{dis}}$  suggest that the reaction initiates from the LMCT state corresponding to the  $5p(\text{I}) \rightarrow \sigma^*_{\text{Sn}-\text{I}}$  absorption.<sup>45</sup> Nevertheless, the product distributions in the polar and nonpolar media differ with  $\text{I}_2$  and  $(\text{CH}_3)_6\text{Sn}_2$ , indicating homolytic cleavage in hexane, whereas  $\text{I}_3^-$ ,  $\text{I}_2$ ,  $(\text{CH}_3)_6\text{Sn}_2$ , and  $(\text{CH}_3)_3\text{Sn}-\text{O}-\text{Si}\equiv$  suggest homolytic and heterolytic cleavage in hydroxylated media. A priori, heterolytic cleavage appears to be consistent with the LMCT character of the reactive excited state, but analogy to transition metal photochemistry suggests that the reaction would lead to the reduced metal and  $\text{I}_2$  formation, not  $\text{I}_3^-$ .<sup>1b</sup> The isomer shift exhibited by  $(\text{CH}_3)_3\text{Sn}-\text{I}$  in hexane, 1.28 mm/s, indicates the Sn is partially positive, implying the Sn–I bond is polarized, i.e.,  $\text{Sn}^{\delta+}-\text{I}^{\delta-}$ .<sup>48,50</sup> The smaller isomer shift for  $(\text{CH}_3)_3\text{SnI}$  adsorbed onto PVG and the larger quadrupole splitting (Table 1) indicate that the formation of the surface-bound adduct increases ground-state polarization with the tin becoming more positive and the iodide more negative.<sup>50</sup> The maximum polarization appears to occur in ethanol, where the  $(\text{CH}_3)_3\text{SnI}-\text{OHC}_2\text{H}_5$  adduct reacts spontaneously with  $\text{I}_2$  to form a  $[(\text{CH}_3)_3\text{Sn}(\text{OHC}_2\text{H}_5)^+, \text{I}_3^-]$  ion pair. These increases in ground-state polarization may account for the larger molar extinction coefficients in alcohol. In hexane, for example, the molar extinction coefficient for the LMCT transition is  $3.45 \times 10^3 \text{ M}^{-1} \text{ cm}^{-1}$ , while in ethanol, the molar extinction coefficient for the LMCT transition is  $1.54 \times 10^4 \text{ M}^{-1} \text{ cm}^{-1}$ . In each medium, the ground state of the molecule is polarized and 254 nm excitation populates an LMCT state. Charge transfer from the halogen to the tin reduces polarity and creates a more uniform charge distribution in the excited state, which, when coupled with specific distortion(s), could be the reason homolytic cleavage occurs from an LMCT state. In fact, recent CASSCF/MS-CASPT2 calculations on the tetrahedral form of the molecule show that the state corresponding to the  $5p(\text{I}) \rightarrow \sigma^*_{\text{Sn}-\text{I}}$  transition is dissociative with respect to the Sn–I coordinate, leading directly to radical products within 100 fs.<sup>45</sup>

Scheme 1



Since homolytic cleavage is consistent with LMCT state, the formation of  $I_2$  and  $(CH_3)_6Sn_2$  in hexane and on the glass surface suggests homolytic cleavage ( $k'$  in Scheme 1) as the primary photochemical event in each medium. In hexane,  $32 \pm 5\%$  of the  $(CH_3)_3Sn^{\bullet}$  and  $I^{\bullet}$  radicals couple to form  $(CH_3)_6Sn_2$  and  $I_2$ . On the more polar surface of the glass, however, a fraction of the radicals undergo secondary reactions leading to  $(CH_3)_3Sn-O-Si\equiv$  and  $I_3^-$ . Recent studies of alkyl halides in polar solvents show that photolysis yields products indicative of the formation of both radical pairs and ion pairs. Peters and co-workers report that both radical pairs and ions pairs are created from a common excited state in diarylmethyl chlorides.<sup>55</sup> The radical pair does not adiabatically couple to re-form the carbon–chlorine bond but decays by electron transfer to form a contact ion pair.<sup>53</sup> Pincock and co-workers suggest that the decay of radical pairs generated in the photolysis of 1-naphthylmethyl esters of phenylacetic and 3-phenylpropanoic acid occurs through an electron-transfer process because the rate of decay of the radical pair is dependent on the polarity of the solvent.<sup>56</sup> Since Mossbauer spectra indicate formation of the surface-bound  $(CH_3)_3Sn-O-Si\equiv$ , electron transfer between the radical primary products,  $k_{th}$ , is thought to be followed by proton transfer,  $k_2$ , with the HI reacting with  $I_2$  to form  $I_3^-$ .

The data do not provide a quantitative estimate of the fraction of radical pairs undergoing electron transfer on the glass surface. Qualitatively, however, assuming similar recoilless fractions for each complex, the relative intensities

of the Mossbauer absorptions of  $(CH_3)_6Sn_2$  and  $(CH_3)_3Sn-O-Si\equiv$  suggest that it is small. A similar mechanism appears to occur in ethanol except that, in this case, the majority of  $I_3^-$  formed arises from the thermal reaction of  $I_2$  with the  $(CH_3)_3SnI-OHC_2H_5$  adduct to form the  $[(CH_3)_3Sn-OHC_2H_5^+, I_3^-]$  ion pair. From the materials point of view, the species leading to gradient index formation is  $(CH_3)_3Sn-O-Si\equiv$ , which decomposes to tin oxide during the subsequent heating and consolidation of the glass matrix.

## Conclusion

Although  $(CH_3)_3SnI$  exists as a discrete tetrahedron in hexane and as a five-coordinate adduct on the surface of porous glass and in alcohol, the photochemistry arises from the same LMCT state and population of this state leads to homolytic cleavage as the primary photoprocess in each medium. Radical coupling is the dominant secondary thermal event in nonpolar media, whereas a fraction of the radical pairs undergo subsequent thermal electron transfer leading to  $I_3^-$  and the surface-bound  $(CH_3)_3Sn-O-Si\equiv$  on the more polar surface of the glass. In ethanol,  $I_3^-$  arises principally from a secondary thermal reaction in which  $I_2$  from the homolytic cleavage reacts with the ethanol adduct  $(CH_3)_3SnI-OHC_2H_5$  to form a  $[(CH_3)_3Sn OHC_2H_5^+, I_3^-]$  ion pair.

**Acknowledgment.** Support of this research by the National Science Foundation (Grants DMR-9314033 and CHE-0079040), the Department of Defense/Air Force Office of Scientific Research (Grant F49620-94-1-0209), the Petroleum Research Foundation administered by the American Chemical Society, and the New York State Science and Technology Foundation through the CUNY Ultrafast Photonics Materials and Applications Center for Advanced Technology is gratefully acknowledged. H.D.G. thanks Corning, Inc. for samples of code 7930 porous Vycor glass.

IC010051C

- (53) (a) Iler, R. K. *The Chemistry of Silica*; Wiley-Interscience: New York, 1979; pp 551, 622–714. (b) Brinker, C. J.; Scherer, G. W. *Sol-Gel Science; the Physics and Chemistry of Sol-gel Processing*; Academic Press: San Diego, CA, 1990; Chapter 9.
- (54) (a) Buckles, R. E.; Yuk, J. P.; Popov, A. I. *J. Am. Chem. Soc.* **1952**, *74*, 4379. (b) Popov, A. I.; Brinker, K. C.; Campanar, L.; Renehart, R. W. *J. Am. Chem. Soc.* **1951**, *73*, 514.
- (55) Lipson, M.; Deniz, A. A.; Peters, K. S. *J. Am. Chem. Soc.* **1996**, *118*, 2992.
- (56) Pincock, J. A.; Wedge, P. J. *J. Org. Chem.* **1994**, *59*, 5587.